

# Atomic Emission Spectroelectrochemistry as A Sensitive Technique for Trace and Ultra- Trace Determination of Metal Species

Mohammad Mahdi Doroodmand\*, Fatemeh Ghasemi

Department of Chemistry, College of Sciences, Shiraz University, Shiraz 71454, Iran.

\*Corresponding author: E-mail: doroodmand@shirazu.ac.ir (M. M. Doroodmand), Tel: +98-71-36137152, Fax: +98-71-36460788

**Abstract**— A novel and sensitive detection system is introduced based on atomic emission spectroelectrochemistry (AESE) inside flame for rapid determination of alkali and some alkaline earth metal ions in the tested samples of rain and drinking water. In this design, the triangular-shaped (inverted Y) three-electrode system consists of two stainless steel rods as the working and counter electrodes, and a brass rod as the pseudo-reference electrode inside the H<sub>2</sub>-air flame. The inter-electrode distance was set to 2.0 mm using two micrometers, connected to the counter and reference electrodes. The atomic emission of metal species such as alkali and alkaline earth ions was selected as the detection system during applying a fixed DC potential to the electrode system. In this system, the analyte was introduced into the flame as the electrolyte via formation of aerosols using a sonicator through the flow of N<sub>2</sub> as a carrier gas. The mixture of H<sub>2</sub> and air was introduced into the flame by a capillary hole along the working electrode. To analyze each metal ion, parameters such as type and quantity of supporting electrolyte, kind of electrodes, inter-electrode distance, applied potential, and the flow rates of H<sub>2</sub>, air, N<sub>2</sub>-were optimized using the one-at-a-time method. According to the figures of merit under the optimized condition, this system has linear dynamic ranges of 0.3-8.0, 0.26-9.6, 0.65-8.0, 64.0-192.0, 80.0-400.0, and 160.0-800.0 μg mL<sup>-1</sup> for Li<sup>+</sup>, Na<sup>+</sup>, K<sup>+</sup>, Cs<sup>+</sup>, Ca<sup>2+</sup>, and Ba<sup>2+</sup>, respectively. Regarding 90% of maximum response (t<sub>90</sub>), the response time was estimated to be 7.0 s. The reliability of the sensor was also evaluated via determination of sodium and potassium in different wastewater samples. Compared to the flame photometry, no significant interfering effect was observed during spiking at least 200-fold excess of some foreign species such as alkali and alkaline earth metal ions to their standard solutions. An appropriate correlation was evaluated during the comparison between the results of this method and those estimated using inductively coupled plasma revealing the reliability and acceptance of this process. The validity of this method has also been evaluated via estimation of the recovery percentages. Compared to the atomic

absorption/emission flame spectrometric techniques, the significant advantages of this AESE system include: I) more sensitive emission during applying the electrical potential in a cool flame such as H<sub>2</sub>-air; II) more improved detection limit and wider linear dynamic range, and III) the cheapness of this method.

**Keywords**— Atomic Emission, Spectroelectrochemistry, Alkali Metal, Earth Metal.

## I. INTRODUCTION

Accurate measurement of cations like Li<sup>+</sup>, Na<sup>+</sup>, and K<sup>+</sup> is highly essential in various real environments such as environmental, industrial, clinical, and biological samples [1,6]. According to the literature, different analytical methods such as atomic absorption/emission spectrometry (AAS/AES) [7,8] inductively coupled plasma (ICP) [9], molecular/atomic fluorescence spectrometry (MFE/AFS) [10], ion-exchange chromatography [11] as well as electrochemical techniques like potentiometry using ion-selective electrodes [12, 13], voltammetry [14] and electro analysis [15] [16] have been reported. However, these analytical techniques in spite of their advantages such as considerable sensitivity [17], occasionally suffer from problems including low improved detection limit, narrow linear range and/or chemical/optical interferences [17, 18].

For instance, AAS, for detection and determination of alkali metals, does not have enough sensitivity [17]. Besides the problems such as self-absorption, this technique is sometimes limited due to the necessity of background correction during measuring the absorbance intensity [17]. Moreover, scientific skills, such as precise control of temperature, are needed during operation of the AES for the determination purposes. Furthermore, at the best conditions of linear ranges during direct and general determination of atomic species inside the flame is often in the range of μg mL<sup>-1</sup> levels [17].

In the ICP analysis, regardless of its acceptable detection limit (at ng mL<sup>-1</sup> levels) and possibility for simultaneous detection purposes, some challenges have limited its applications including high cost of the pure argon,

chemical/optical interferences, lack of portability as well as occasionally moderate linearity [9, 17, 19, 20]. Nevertheless, the sensitivity index in fluorescence spectroscopy is limited to the fluorescence quantum yield [21] which is sometimes small, especially for the forbidden transitions due to the effective role of phenomena such as self-absorption, scattering, intersystem crossing and quenching. [21]. Limitations in the electrochemical techniques including fouling the electrode system and the electrochemical interferences may provide the demand for introduction of new methods.

In the flame photometry (atomic emission spectrometry), the emission intensity depends on the population of electrons excited by the heat of the flame as an atomizer. This method is often applicable for qualitative and quantitative analyses of several alkali and alkaline earth metals. Compared to the AAS, higher sensitivity is considered as the most important advantages of this analytical technique. The calibration sensitivity of this analytical technique can be controlled by the operator via the definition of a calibration curve during the introduction of the blank solution and the dark current adjustment (zero adjustments) of the detector. This procedure is then finalized by the introduction of a concentrated standard solution in the linear range and controlling the calibration sensitivity of the method. However, for more confidence about the presence of the concentrated standard solution in the linear range of the calibration curve, it is recommended to introduce some different standard solutions sequentially. This procedure is attributed to the absolute characteristic of the emission intensity, compared to the relative property of transmittance and absorbance, which is evaluated vs. the intensity of an optical source in the AAS. Therefore, different calibration sensitivities can be defined by the operator. These characteristics of the flame photometric technique cause a precise focus on the limitations of detection and quantity (LOD, LOQ) during the evaluation of figures of merit of this method.

In the AES, controlling the temperature is very important to excite electrons as large as possible. Low temperatures of the flame limit the pollutions of excited atomic species inside the analyzing volume (flame), whereas higher temperatures of the analyzing volume oxidize the atomic species into their cationic forms. Therefore, precise controls of the flame, as the needs to have scientific knowledge of this phenomenon, are considered as the most serious limitations of this technique.

To enhance the temperature, often more oxidizing agents (supports) such as pure oxygen, nitrous oxide or air are recommended during using acetylene as fuel. Due to the importance of the flashback in the pre-mixed burner, sometimes total-consumption (turbulent) burner is recommended at high temperatures. This instrumental limitation brings about the turbulence analyzing volume.

This problem motivates a noisy emission response that restricts the reproducibility (precision) of this analytical method seriously. All these problems also make the high sensitivity of the method and provide the condition for the serious influence of the interfering effects of some anionic and cationic species. This challenge is more considerable especially during the formation of a sophisticated matrix for the real and standard samples via sweeping the matrix of the real sample by addition of radiation buffer using the mixture of concentrated species probably presented in the real sample. Therefore, serious modifications are needed to solve the existing chandelles of the flame photometry. It seems that combination of reaction-oriented electrochemistry with species-focused spectroscopy in the spectroelectrochemistry brings about advantages such as the possibility to analyze complex species through single and multiple electron-transfer processes and redox reactions. Coupling the electrochemistry with the spectroscopy can provide a new analytical system with maximum advantages as well as minimum limitations of the two abovementioned methods. Although the basic background of this technique is not so innovative, the application of this field inside the flame as both the atomizer and the electrolyte medium has not been applicable [22]. This problem is related to the intrinsic challenges of the flame such as i) low electrical conductivity; ii) nonhomogeneous thermal matrix, and iii) high turbulent [22-25] that bring about an insensitive and very noisy voltammogram. Solving these problems leads to have a sensitive detection system for metal determination purposes. To do so, in this study a new system has been introduced for sensitive and selective determination of metal alkali species such as  $\text{Li}^+$ ,  $\text{Na}^+$ ,  $\text{K}^+$ ,  $\text{Ba}^{2+}$ , and  $\text{Ca}^{2+}$  using atomic emission spectroelectrochemistry (AESE).

## II. EXPERIMENTAL

### 2.1 Reagents

The entire reagents have been from their analytical grades. Stock solutions ( $1000.0 \mu\text{g mL}^{-1}$ ) of  $\text{Na}^+$ ,  $\text{K}^+$ ,  $\text{Cs}^+$ ,  $\text{Li}^+$ ,  $\text{Ca}^{2+}$ , and  $\text{Ba}^{2+}$  were prepared via individually dissolving 2.5420, 1.9070, 1.2667, 6.1070, 3.9465, and 1.7785 g dried salt of NaCl (Merck, Darmstadt, Germany), KCl (Merck, Darmstadt, Germany), CsCl (Fluka), LiCl (Merck, Darmstadt, Germany),  $\text{Ca}(\text{CH}_3\text{COO})_2$  (Merck, Darmstadt, Germany), and  $\text{BaCl}_2 \cdot 2\text{H}_2\text{O}$  (Fluka), respectively in 1000 mL volumetric flask using deionized water as solvent. A 1000-mL solution of  $\text{H}^+$  (0.45 M) was also prepared via dissolving 37.2 mL HCl (37% W/W, specific weight: 1.19, Merck, Darmstadt, Germany) as supporting electrolyte and diluting to the mark using deionized water.

### 2.2 Instrumentation

The detail of the designed AESE system is based on a novel flame-based electroanalyzer (FBE) system, fabricated for selective determination of each alkali and alkaline earth

metal ions such as  $\text{Li}^+$ ,  $\text{Na}^+$ ,  $\text{K}^+$ ,  $\text{Cs}^+$ ,  $\text{Ca}^{2+}$ , and  $\text{Ba}^{2+}$ . The schematic of the AESE instrumentation system is shown in Fig. 1. In the designed AESE, a triangular (inverted Y) - shaped three-electrode system was utilized inside  $\text{H}_2$ -air flame as analyzing volume. Each tip of the three-electrode system was considered as the vertex of a triangular. The counter electrode includes a stainless steel rod (Tip: 310, diameter: 2.0 mm, length 25.0 mm). The working electrode consists of two concentric stainless steel tubes. The outer tube was 12.0 mm OD, 10.0 mm ID, and the inner is a capillary tube with 3.0 mm OD tube that plays a role as the working electrode. The end of the capillary tube is positioned ~4.0 cm shorter than the inside tip of the outer tube. The inner capillary tube transfers air and the outer carries hydrogen gas. A brass rod (diameter: 3.0 mm, length 25.0 mm) as pseudo-reference electrode was also situated inside the  $\text{H}_2$ -air flame (hydrogen:  $\text{H}_2$  cylinder, Isfahan Petrochemical Company, purity: 99.996%, air: air pump, model: PYE UNICAM Ltd). As shown in Fig. 1, the working electrode was fixed to the base of the system, whereas the positions of each reference and counter electrodes were controlled vs. the working electrode using two independent hand-controller micrometers (model: Starrett). In this design, the potential value ranged from 0.0 to 250.0 V was generated using a function generator (model: 3390). The applied potential as well as the emission intensity of the atomic-emission spectrometer (model: PYE UNICAM SP9) were simultaneously measured using two AVO meters (model: AT-9995) and were reported directly to a PC via the USB port.

To introduce the samples into the flame, a glass reaction tubing cell with 20.0 mL volume was fabricated. A sonicator (model: MIST MAKER, frequency: 500-KHz) was also positioned at the bottom of the solution-containing tubing cell for the generation of aerosols. The generated aerosols were then carried into the flame through a Tygon tubing (internal diameter: 3.0 mm) using  $\text{N}_2$  gas ( $\text{N}_2$  cylinder, purity: 99.9, Parsbaloon, Iran, Shiraz).

### 2.3 Activation of the electrode systems

Stainless steel electrodes, particularly those never used before for the electrochemical experiments, are often found to contain the impurity of some metals such as Cr at their matrix when submerged into the electrolyte solution [26]. These impurities can be removed by pretreating the electrode in the  $\text{H}_2$ -air flame for ~ 3.0 min during several times before obtaining the desired baseline. At this condition, black body radiations (Red radiations) are clearly emitted from the counter electrode. This process, therefore, leads to an electrode with a high active surface area.

### 2.4 Procedure

To determine each alkali and alkaline earth metal ions such as  $\text{Li}^+$ ,  $\text{Na}^+$ ,  $\text{K}^+$ ,  $\text{Cs}^+$ ,  $\text{Ca}^{2+}$ , and  $\text{Ba}^{2+}$  the flow rates of

$\text{H}_2$ , air, and  $\text{N}_2$  were set based on the values reported in Table 1. For the analytical purpose, the surfaces of the working, reference, and counter electrodes were polished using a piece of paper sand (Type: P 2000). The same distances (2.0 mm) were set between the electrodes to provide a triangular (inverted Y) shape. A fixed DC potential vs. the pseudo ref. electrode was then applied to the working electrode for each of the tested analytes at a maximum wavelength as reported in Table 1. To introduce the sample into the flame, a fixed volume (10.0 mL) of HCl solution (0.45 M) containing an analyte or a standard solution was inserted into the solution-containing tubing cell. After turning on the sonicator for approximately 5 seconds, the aerosols were introduced to the flame during a 7 s time interval, and the emission intensity was measured and saved in the PC.

### 2.5 Recommended procedure for real sample analyses

The application of the recommended method is adapted for determination of alkali ions such as  $\text{Na}^+$  and  $\text{K}^+$  in various rain and drinking water samples. To do so, the samples were individually diluted for ~12 times and determined using standard addition method. The reliability of this method was evaluated using ICP (model: VARIAN VISTA-PRO).

## III. RESULTS AND DISCUSSION

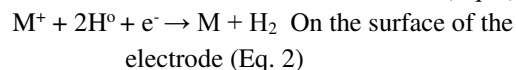
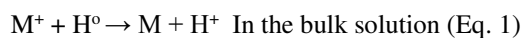
In this study, a novel FBE was designed for selective determination of alkali and alkaline earth metal ions such as  $\text{Li}^+$ ,  $\text{Na}^+$ ,  $\text{K}^+$ ,  $\text{Cs}^+$ ,  $\text{Ca}^{2+}$ , and  $\text{Ba}^{2+}$ . To achieve an acceptable selectivity during the detection of metal species inside the flame, the emission intensity was measured by applying potential to the  $\text{H}_2$ -air flame.

Parameters which have strong influences on the measuring emission during applying the potential to the  $\text{H}_2$ -air flame include the potential values applied to the electrodes; the flow rates of  $\text{H}_2$ , air and  $\text{N}_2$  gases; the volume of the solution inside the cell; injection time of the sample introduced to the flame; the kind of acid (supporting electrolyte) as the source of radical hydrogen ( $\text{H}^\circ$ ) in the flame; ionic strength of the solution; and the distance between the electrodes inside the  $\text{H}_2$ -air flame. All the parameters were optimized by the one-at-a-time method. The working conditions for determination of the emission intensity by the spectrophotometer have been similar to the analytical methods recommended in different catalogs such as "Varian and Agilent Company" [27].

For this purpose, standard solutions of  $\text{Li}^+$  ( $5.0 \mu\text{g mL}^{-1}$ ),  $\text{Na}^+$  ( $5.0 \mu\text{g mL}^{-1}$ ),  $\text{K}^+$  ( $5.0 \mu\text{g mL}^{-1}$ ),  $\text{Cs}^+$  ( $80.0 \mu\text{g mL}^{-1}$ ),  $\text{Ca}^{2+}$  ( $280.0 \mu\text{g mL}^{-1}$ ), and  $\text{Ba}^{2+}$  ( $240.0 \mu\text{g mL}^{-1}$ ) have individually been utilized as selected probes. These selections were based in the middle region of the linear range initially estimated at maximum wavelengths of 670.8, 589.0, 766.0, 852.1, 422.7, and 553.6 nm for each of  $\text{Li}^+$ ,  $\text{Na}^+$ ,  $\text{K}^+$ ,  $\text{Cs}^+$ ,  $\text{Ca}^{2+}$ , and  $\text{Ba}^{2+}$  ions, respectively [27].

Fig. 2 shows the emission intensity during applying potential to the electrode system throughout the introduction of the cationic species ranged between  $\sim 0.0$  and  $-200.0$  V (vs. the reference electrode). As clearly shown, the less sensitive emission intensity was observed at low potentials (vs. the reference electrode). Therefore, to have maximum sensitivity, fixed DC potentials including  $-100.0 \pm 1.0$ ,  $-90.0 \pm 1.0$ ,  $-50.0 \pm 1.0$ ,  $-90.0 \pm 1.0$ ,  $-100.0 \pm 1.0$ , and  $-160.0 \pm 1.0$  V have been applied to the electrode system for the detection of the following species such as Li, Na, K, Cs, Ca and Ba, respectively of the fabricated AESE. The effect of applied potential to the flame photometric system has been shown in the histogram of Fig. 3. The significant sensitivity of this method is assessed compared to the general flame photometry (atomic emission spectroscopy).

Another factor that plays an important role in the sensitivity of the system for selective detection of each ion is the flow rates of  $H_2$  and air. To optimize these parameters, the response of the emission system has been evaluated during the introduction of different flow rates of  $H_2$  and air using two independent flow controllers. The results are displayed in Figs. 4 and 5. As expected, the stoichiometry of hydrogen vs. air plays an important role in the degree of the sensitivity. Whenever the stoichiometry of hydrogen vs. air is low, the flame was oxidized and the alkali species were mostly stable in their cationic forms. In the reverse condition (i.e. reducing flame), these species are often presented inside the flame in their atomic forms. According to the results (Fig. 4), maximum sensitivity was therefore observed at  $H_2$  flow rates of 683, 560, 560, 560, 683, and 560  $mL\ min^{-1}$  for  $Li^+$ ,  $Na^+$ ,  $K^+$ ,  $Cs^+$ ,  $Ca^{2+}$  and  $Ba^{2+}$  ions, respectively. As shown in Fig. 4, the sensitivity at lower flow rates of  $H_2$  is poor; this is probably due to the stability of metal species such as sodium ions. Moreover, low quantity of  $H^0$  inside the flame prevents the reduction of cations into the metallic form; this is probably based on the following reactions (Eqs. 1 and 2):



The trace quantity of alkali ions is therefore reduced on the surface of the electrode during the formation of the metal species with zero oxidation state. Whereas, the reverse behavior is observed when dealing with high flow rates of  $H_2$ ; this is probably due to the effective role of temperature on the stability of sodium ions. Consequently, the  $H_2$  flow rate is effective because of its enhancing effect on the sensitivity of the flame. according to the results (Fig. 5), maximum sensitivity is observed at the air flow rates of 142, 25, 101, 4, 313, and 419  $mL\ min^{-1}$  for  $Li^+$ ,  $Na^+$ ,  $K^+$ ,  $Cs^+$ ,  $Ca^{2+}$ , and  $Ba^{2+}$  ions, respectively. It seems that at lower flow rates, the turbulence behavior of the flame is the main reason for low sensitivity. On the contrary, at high-flow rates of the air, the oxidizing behavior of the flame again lowers the

sensitivity. As clearly shown (Figs. 4, 5), the flow rates of  $H_2$  and air, compared to other radicals such as  $O^0$  or  $^0OH$  as shown in Eqs. 1 and 2, clearly point to the effective role of  $H^0$ .

To optimize the quantity of samples introduced to the flame via formation of aerosols, parameters such as time duration of the injection, the volume of the reagent in the solution-containing tubing cell, and the flow rate of  $N_2$  as carrier gas have been optimized. The flow rates of  $N_2$  should be set to maximize the quantity of the samples introduced into the flame during the laminar mode of the flame. Therefore, the flow rate of 2.37  $mL\ min^{-1}$  has been selected as the optimum value for  $N_2$  as the carrier gas.

To control the direction of the mass transfer process, it is necessary to control the surface of the electrode system. In this regard, it is recommended to polish the surface of the electrode system prior its use in the electrochemical processes [28]. In addition, during the use of electrode system in the electrochemical process, the electrodes are often fouled and sometimes poisoned by some impurities such as some metal ions inside the flame as an electrolyte during some physic/chemical processes like adsorption, absorption or chemical reactions [28]. To solve these problems, it is recommended to polish the electrode surface using a piece of sandpaper (Type: 2000) through a circular motion until the formation of a disk electrode with a flat and smooth surface. The polishing process also leads to have an electrochemical system with higher sensitivity and more acceptable reproducibility. Thus, this process allows the electrode to remain reusable during several analyses. The polishing process often takes a short time, for example only several minutes (maximum 3 min), for a hard electrode made of stainless steel during each 10-time analysis.

The time duration of the injection (injection time) has also been optimized during the introduction of a significant quantity of the sample into the flame. To optimize the flow rate as well as the injection time of  $N_2$  as a carrier gas, parameters such as the shape of the cell as well as the volume of the electrolyte inside the cell were also evaluated. Regarding the direct observations, an appropriate volume of the electrolyte for the generation of stable aerosols was estimated to be  $\sim 10$  mL. Suitable injection time is also set to  $\sim 7$  s.

In the electrochemical process, supporting electrolyte controls the mass transfer of the electroactive species based on the diffusion process. To select the supporting electrolyte in this study, the effect of some acids such as HCl,  $HNO_3$ , and  $H_2SO_4$  was evaluated. This selection was based on the effective role of these species during the formation of  $H^0$  from  $H^+$ . Therefore, the effect of acid as the source of  $H^0$  on the emission intensity was investigated in detail. In this regard, a standard solution of  $Na^+$  with 3.0  $\mu g\ mL^{-1}$  concentration has been investigated in different acidic environments (0.45 M) and compared to the neutral water.

Based on the results shown in Fig. 6, the highest emission intensity is observed HCl solution with 0.45 M concentration. This is attributed to the effective behavior of HCl during the generation of H<sup>o</sup> inside the H<sub>2</sub>-air flame.

### 3.1 Analytical figures of merit

The calibration curves related to each of alkali and alkaline earth ions have been illustrated in Fig. 7. As shown, the introduced method is suitable for the determination of alkali and alkaline earth metal ions with linear dynamic range between 0.30 and 8.0 (correlation coefficient (R)= 0.984), 0.26-9.6 (R= 0.993), 0.65-8.0 (R= 0.997), 65.0-192.0 (R= 0.989), 80.0-400.0 (R= 0.994), and 160- 800 µg mL<sup>-1</sup> (R= 0.996) for Li<sup>+</sup>, Na<sup>+</sup>, K<sup>+</sup>, Cs<sup>+</sup>, Ca<sup>2+</sup>, and Ba<sup>2+</sup>, respectively. The detection limit was also defined as the concentration of each metal giving a signal equal to the blank signal plus triple values of the standard deviation of the blank. Based on this definition, the limits of detection have been found as 0.07, 0.09, 0.04, 40.0, 60.0, and 70.0 µg mL<sup>-1</sup> for Li<sup>+</sup>, Na<sup>+</sup>, K<sup>+</sup>, Cs<sup>+</sup>, Ca<sup>2+</sup>, and Ba<sup>2+</sup>, respectively.

The sensitivity of this method is assessed according to the slopes (calibration sensitivity) of the calibration curves (Fig. 7). These parameters have been estimated to be 1.972, 1.21, 1.807, 0.073, 0.005, and 0.005 (a.u.) for Li<sup>+</sup>, Na<sup>+</sup>, K<sup>+</sup>, Cs<sup>+</sup>, Ca<sup>2+</sup>, and Ba<sup>2+</sup>, respectively. The high sensitivity of this method is strongly correlated to the capability of the designed AESE. According to the results, relative standard deviations (n = 8) were estimated to be 7.0, 5.0, 6.0, 11.0, 6.0, and 7.0 % for Li<sup>+</sup>, Na<sup>+</sup>, K<sup>+</sup>, Cs<sup>+</sup>, Ca<sup>2+</sup>, and Ba<sup>2+</sup>, respectively. Consequently, reproducible results are obtained during at least 8 replicate analyses of a fixed concentration of Li<sup>+</sup>, Na<sup>+</sup>, K<sup>+</sup>, Cs<sup>+</sup>, Ca<sup>2+</sup>, and Ba<sup>2+</sup>.

To evaluate the selectivity of this method for the detection and determination of alkali and alkaline earth metals, the effect of some foreign ionic species was also evaluated in detail. To do so, at least 200-fold excess of some kind of ionic species including some alkali and alkaline earth metal ions were spiked into the alkali standard solutions like 4.8, 8.0, and 8.0 µg mL<sup>-1</sup> for Na<sup>+</sup>, K<sup>+</sup>, and Li<sup>+</sup>, respectively, then evaluated in detail. Based on the results, no significant change is observed in the emission intensity revealing high selectivity of this method. The acceptable selectivity of this method is probably attributed to some different phenomena such as i) the effect of aerometry during applying selective reduction potential, ii) the emission intensity measured at a maximum wavelength of each ionic species, and iii) catalytic behavior of H<sup>o</sup> during the electrochemical reduction on the surface of the working electrode. Table 2 shows selected figures of merit for analysis of Li<sup>+</sup>, Na<sup>+</sup>, K<sup>+</sup>, Cs<sup>+</sup>, Ca<sup>2+</sup>, and Ba<sup>2+</sup> based on the designed AESE. According to the results, significant improvements are observed in some figures of merit such as sensitivity compared to the general AES.

### 3.2 Real sample analysis

The validation of the method was evaluated by an analytical test for sodium and potassium ions through the comparison between this technique and ICP as a reference and accepted analytical method, followed by estimation of the absolute error. For this purpose, the standard addition method was used during the replicate analyses of some rain and drinking water samples. Sampling has been performed with regard to the ASTM report [29]. According to the results (Table 3), a partially good agreement has been evaluated by comparing the results of this technique and the ICP revealing the reliability and acceptance of this method.

Further validation of the proposed method was evaluated by estimating the recovery percentages through spiking a fixed standard solution of Na<sup>+</sup> and K<sup>+</sup> into the real sample solution. For this purpose, the emission intensities of both real sample solutions and those spiked with standard solutions were evaluated. The recovery percentages were also estimated according to the following formula:

Recovery percentage =

$$\frac{(\text{Conc. of the spiked metal ion} - \text{Found value for the background})}{(\text{Found value of the spiked metal ion})} \times 100 \quad (\text{Eq. 3}).$$

Based on the results, maximum ±5% deviation has been estimated from the one hundred recovery percentage during the analysis of K<sup>+</sup> and Na<sup>+</sup> in the real sample solutions. This is considered as another acceptable validation for the reliability (validity) of this method.

### 3.3 Comparison with existing methods

Compared to the flame photometry (Table 4), this method has significant advantages. For instance, to the best of knowledge, this study is the first report that adopts H<sub>2</sub>-air flame as cool and green and transparent atomizer for the atomic emission purposes. In comparison with the CO and CO<sub>2</sub> as the main products of the acetylene-based flames, water vapors are the product of the H<sub>2</sub>-air flame. The combination of the flame-based spectrometry with the electrochemical detection system majorly lowers the dependency of the flame photometry to the temperature. This effect not only decreases the need to the scientific skill during operating the flame photometry but also provides the conditions for sensitive and reproducible measuring the atomic intensity through the electrochemical process. The major enhancement is estimated for the sensitivity during the modification of flame photometry with the electrochemical process. The formation of the excited metal species through both cool flame and the electrochemical process majorly enhances the selectivity of this method and significantly lowers the current existing interferences in the flame photometry (general atomic emission spectrometry). Table 4 also summarizes some differences between this method and the previously reported analytical techniques. Based on the comparison, the detection limit of this method

is not comparable with some electrochemical methods such as ion selective electrodes [30]. Some figures of this method have been compared to different chromatographic and spectroscopic techniques. The wider linear range has been estimated for this method in comparison with the AAS. The LOD and LOQ of this method are partially the same as flame photometry. However, more improved detection limit as well as lower detection range is estimated for certain analytical methods such as ICP and ion chromatography. Problems such as high price, a need for the high pure Ar gas in the ICP, fouling the column of the ion chromatography, and/or high time consuming of the ion chromatography are considered as the most serious limitations in comparison with the introduced method. As a result, all of these characteristics point to the cost-effectiveness of this method compared to the existing analytical techniques such as flame photometry.

#### IV. CONCLUSIONS

A sensitive and reproducible method was introduced for rapid detection of some alkali and alkaline earth metal ions such as  $\text{Li}^+$ ,  $\text{Na}^+$ ,  $\text{K}^+$ ,  $\text{Cs}^+$ ,  $\text{Ca}^{2+}$ , and  $\text{Ba}^{2+}$  species using the designed AESE system. This study was the first report in which emission processes were described for the determination of some metal ions in the  $\text{H}_2$ -air flame. The most important advantages of this proposed method, compared to the general flame photometry, may be considered as the independency of the emission intensity to the atomizer flame, selective reduction of metallic species on the surface of the electrode during using  $\text{H}_2$ -air flame as the electrolyte, green and transparent behavior of the  $\text{H}_2$ /air flame, higher selectivity, and less influence of interfering agents. This study was the basic research to evaluate the effects of the electrical potential on the sensitivity of various cationic species inside different flames. Finally, this method can be considered as an acceptable technique as the aim is the selective analysis of alkali and alkaline earth metals.

#### ACKNOWLEDGEMENTS

The authors wish to acknowledge the support of this work by Shiraz University Research Council.

#### REFERENCES

- [1] R. Machado-Vieira, H.K. Manji, C.A. Zarate Jr, The role of lithium in the treatment of bipolar disorder: convergent evidence for neurotrophic effects as a unifying hypothesis, *Bipolar Disord.*, 11 (2009) 92-109.
- [2] Y. Zhang, W.W. Liou, V. Gupta, Modeling of high sodium intake effects on left ventricular hypertrophy, *Comput. Biol. Med.*, 58 (2015) 31-39.
- [3] D. Shin, H.K. Joh, K.H. Kim, S.M. Park, Benefits of potassium intake on metabolic syndrome: The fourth Korean National Health and Nutrition Examination Survey (KNHANES IV), *Atherosclerosis*, 230 (2013) 80-85.
- [4] H.J. Adrogué, N.E. Madias, Sodium and potassium in the pathogenesis of hypertension, *New Engl. J. Med.*, 356 (2007) 1966-1978.
- [5] K.J. Aaron, P.W. Sanders, Role of dietary salt and potassium intake in cardiovascular health and disease: A review of the evidence, *Mayo Clin. Proc.*, 88 (2013) 987-995.
- [6] M. Kuum, V. Veksler, A. Kaasik, Potassium fluxes across the endoplasmic reticulum and their role in endoplasmic reticulum calcium homeostasis, *Cell Calcium*, 58 (2015) 79-85.
- [7] R.J. Wright, T.I. Stuczynski, Atomic Absorption and Flame Emission Spectrometry, In D.L. Sparks et al. (Eds.), *Methods of soil analysis. Part 3: chemical methods*, SSSA, Madison, WI, USA. , 1996, pp. 65-90.
- [8] L.H.J. Lajunen, P. Perämäki, *Spectrochemical Analysis by Atomic Absorption and Emission*, Second ed., Royal Society of Chemistry, Great Britain, Cambridge, UK, 2004.
- [9] C.J. Hardaway, J. Sneddon, E.J. Sneddon, B. Kiran, B.J. Lambert, T.C. McCray, D.Q. Bowser, C. Douvris, Study of selected metal concentrations in sediments by inductively coupled plasma-optical emission spectrometry from a metropolitan and more pristine bayou in Southwest Louisiana, United States, *Microchem. J.*, 127 (2016) 213-219.
- [10] R. Zhang, M. Peng, C. Zheng, K. Xu, X. Hou, Application of flow injection-green chemical vapor generation-atomic fluorescence spectrometry to ultrasensitive mercury speciation analysis of water and biological samples, *Microchem. J.*, 127 (2016) 62-67.
- [11] J.C. Rea, B.S. Freistadt, D. McDonald, D. Farnan, Y.J. Wang, Capillary ion-exchange chromatography with nanogram sensitivity for the analysis of monoclonal antibodies, *J. Chromatogr. A*, 1424 (2015) 77-85.
- [12] X. Zeng, S. Yu, Q. Yuan, W. Qin, Solid-contact  $\text{K}^+$ -selective electrode based on three-dimensional molybdenum sulfide nanoflowers as ion-to-electron transducer, *Sens. Actuat. B: Chem.*, 234 (2016) 80-83.
- [13] J. Shen, S. Gagliardi, M.R. McCoustra, V. Arrighi, Effect of humic substances aggregation on the determination of fluoride in water using an ion selective electrode, *Chemosphere*, 159 (2016) 66-71.
- [14] G.B. Ngassa, I.K. Tonlé, E. Ngameni, Square wave voltammetric detection by direct electroreduction of parnitrophenol (PNP) using an organosmectite film-modified glassy carbon electrode, *Talanta*, 147 (2016) 547-555.
- [15] W. Wang, L. Wang, L. Zou, G. Li, B. Ye, Electrochemical behavior of arctigenin at a novel voltammetric sensor based on Iodide/SWCNTs composite film modified electrode and its sensitive

- determination, J. Electroanal. Chem., 772 (2016) 17-26.
- [16] J.W. Robinson, E.S. Frame, G.M. Frame II, Undergraduate Instrumental Analysis, Six<sup>th</sup> ed., New York: CRC Press, 2014.
- [17] D.A. Skoog, F.J. Holler, S.R. Crouch, Principles of Instrumental Analysis, Six<sup>th</sup> ed., Thomson Brooks/Cole publishing: Philadelphia, 2007.
- [18] J.D. Ingle, S.R. Crouch, Spectrochemical Analysis, Prentice Hall, First ed., Prentice-Hall: New Jersey, 1988.
- [19] A. Montaser, D. Golightly, Inductively Coupled Plasmas in Analytical Atomic Spectrometry, Second ed., A. Montaser, D.W. Golightly (Eds.), Wiley, New York, 1987.
- [20] R. Dahlquist, J. Knoll, Inductively coupled plasma-atomic emission spectrometry: analysis of biological materials and soils for major, trace, and ultra-trace elements, Appl. Spectrosc., 32 (1978) 1-30.
- [21] C.D. Geddes, J.R. Lakowicz, Topics in Fluorescence Spectroscopy.: Advanced Concepts in Fluorescence Sensing: Small Molecule Sensing, Springer-Verlag, Plenum Press, New York, 2005.
- [22] D.J. Caruana, S.P. McCormack, Electrochemistry in flames: a preliminary communication, Electrochem. Commun., 2 (2000) 816-821.
- [23] J.M. Goodings, J. Guo, J.G. Laframboise, Electrochemical diffusion potential in a flame plasma: theory and experiment, Electrochem. Commun., 4 (2002) 363-369.
- [24] D.J. Caruana, S.P. McCormack, Electrochemical redox potential in flame plasma, Electrochem. Commun., 4 (2002) 780-786.
- [25] A. Elahi, D.J. Caruana, Plasma electrochemistry: voltammetry in a flame plasma electrolyte, PCCP, 15 (2013) 1108-1114.
- [26] R.M. Fernández-Domene, E. Blasco-Tamarit, D.M. García-García, J. García-Antón, Effect of alloying elements on the electronic properties of thin passive films formed on carbon steel, ferritic and austenitic stainless steels in a highly concentrated LiBr solution, Thin Solid Films, 558 (2014) 252-258.
- [27] Agilent Technologies, Flame Atomic Absorption Spectrometry - Analytical Methods Part Number 85100009-00. Tenth Edition, Santa Clara, USA, 2012.
- [28] X. Cheng, S.G. Roscoe, Influence of surface polishing on the electrochemical behavior of titanium, Electrochem. Solid-State Lett., 8 (2005) B38-B41.
- [29] R.K. Scott, V.M. Marcy, J.J. Hronas, Technical Standard ASTM, Methods of Test for Sodium and Potassium in Water and Water-Formed Deposits by Flame Photometry (Withdrawn 1988), ASTM D1428-82, DOI.
- [30] K.Y. Chumbimuni-Torres, L.T. Kubota, Simultaneous determination of calcium and potassium in coconut water by a flow-injection method with tubular potentiometric sensors, J. Food. Compost. Anal., 19 (2006) 225-230.
- [31] A.R. Zsigmond, T. Frentiu, M. Ponta, M. Frentiu, D. Petreus, Simple and robust method for lithium traces determination in drinking water by atomic emission using low-power capacitively coupled plasma microtorch and microspectrometer, Food Chem., 141 (2013) 3621-3626.
- [32] B.M. De Borba, M. Laikhtman, J.S. Rohrer, Determination of sodium at low ng/l concentrations in simulated power plant waters by ion chromatography, J. Chromatogr. A, 995 (2003) 143-152.

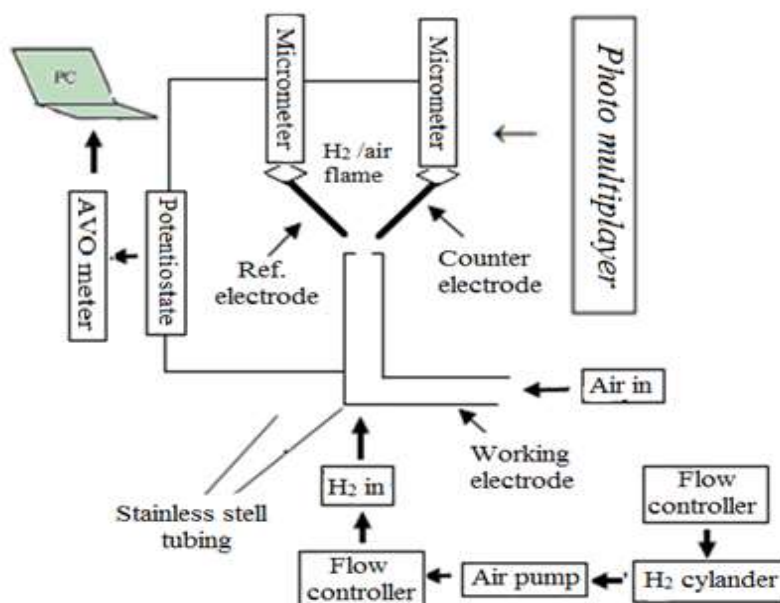


Fig.1: The schematic of the designed atomic emission electro spectroscopic system

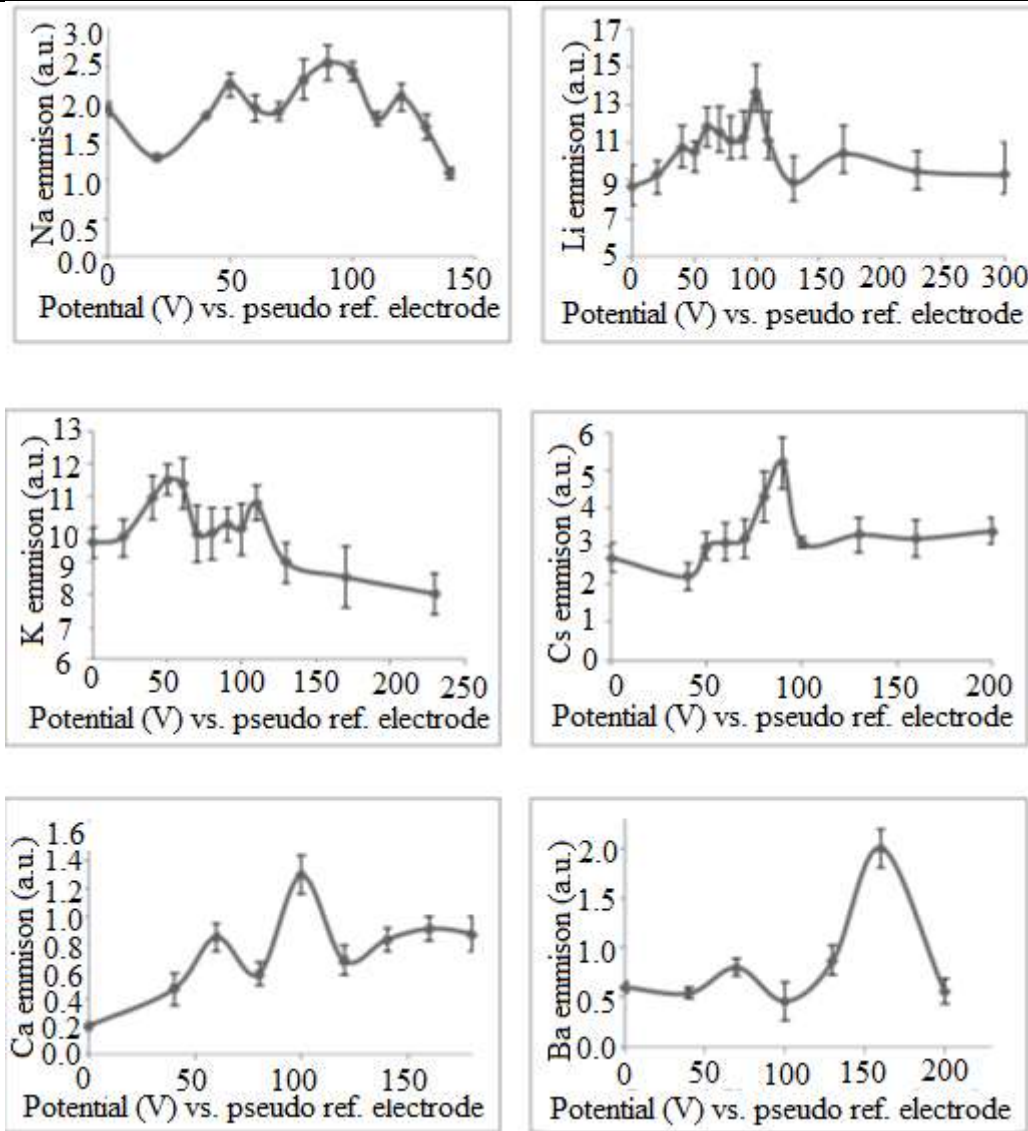


Fig. 2: Diagrams of emission vs. different voltages during analyses of various cationic species

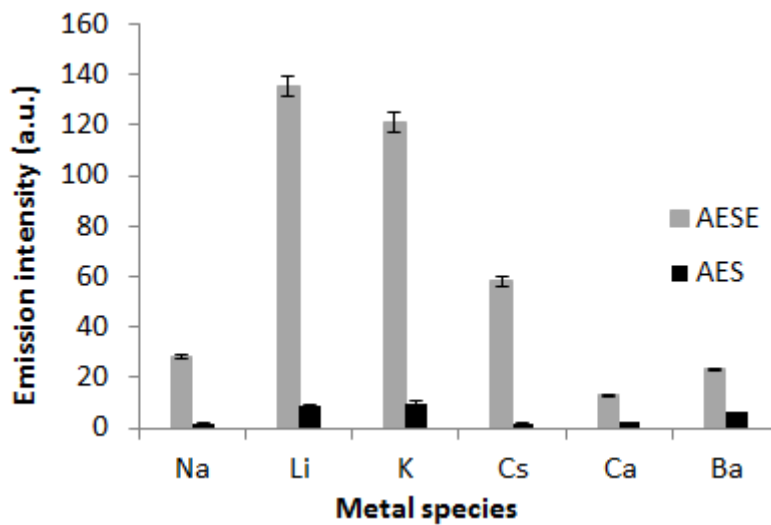


Fig. 3: The effect of applied potential on the emission intensity of atomic emission spectroscopy



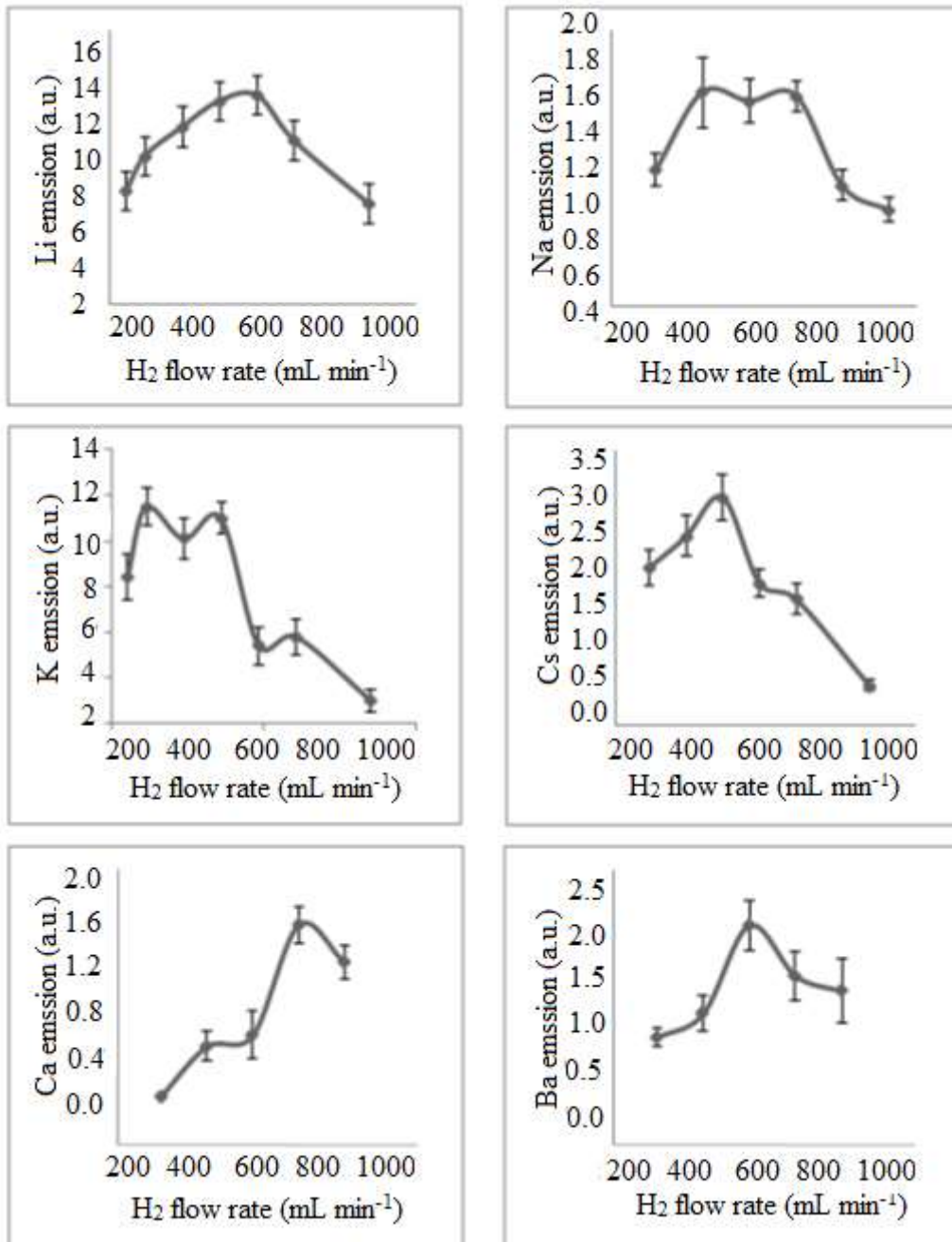


Fig. 4: Diagrams of emission vs. different flow rates of H<sub>2</sub> during individual analyses of various species

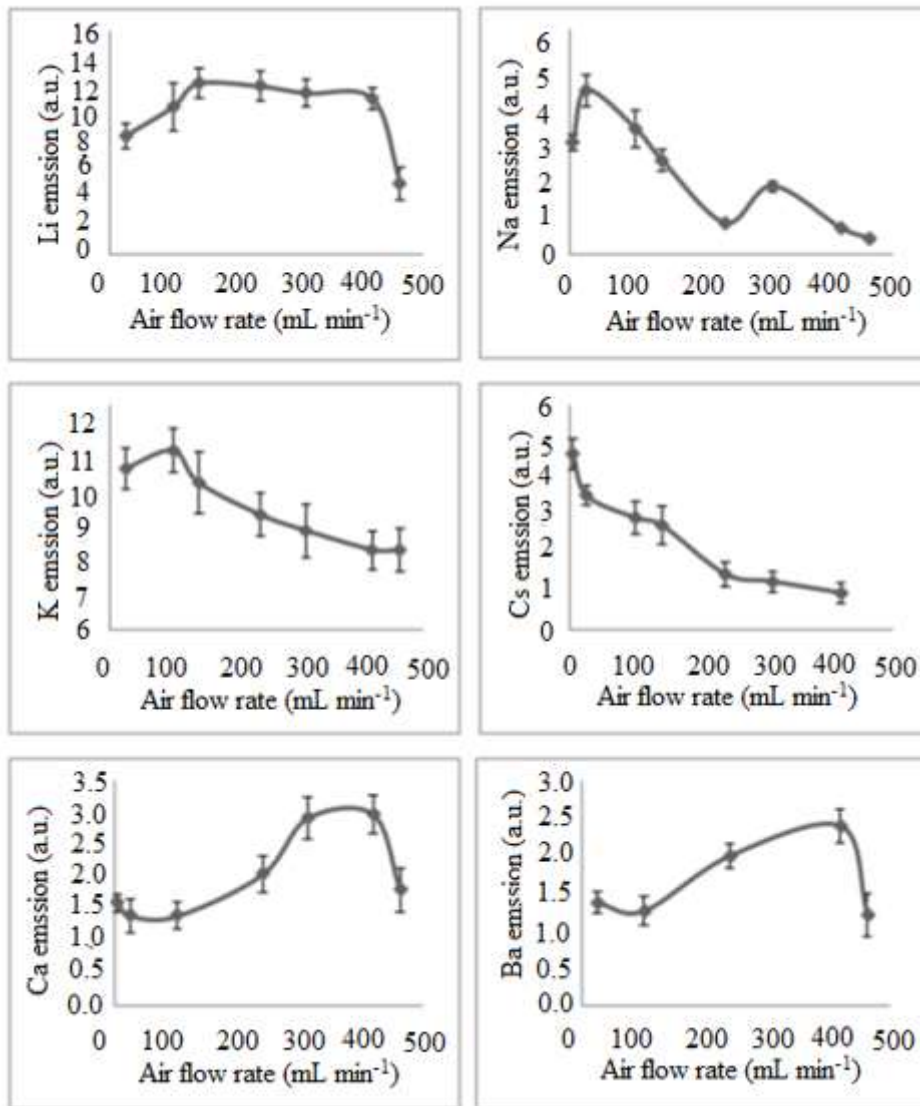


Fig. 5: Diagrams of emission vs. different flow rates of air during individual analyses of various metal ions

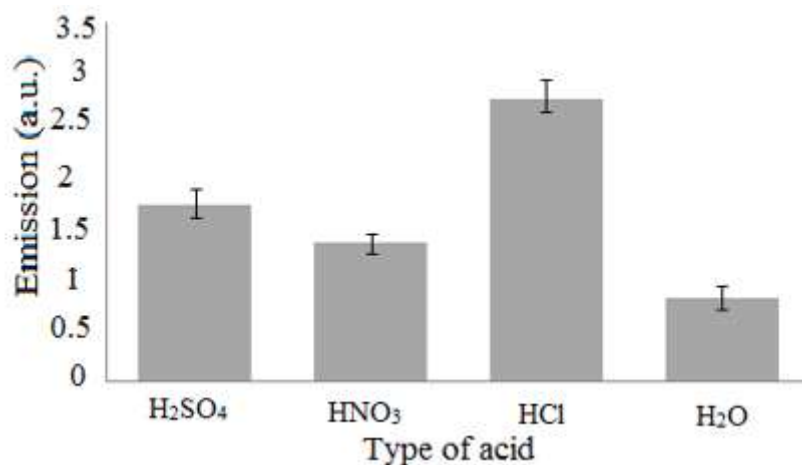


Fig. 6: The effect of various acidic species (0.45 M) as the source of H<sup>+</sup> on the sensitivity of Na<sup>+</sup> (3.0 μg mL<sup>-1</sup>)

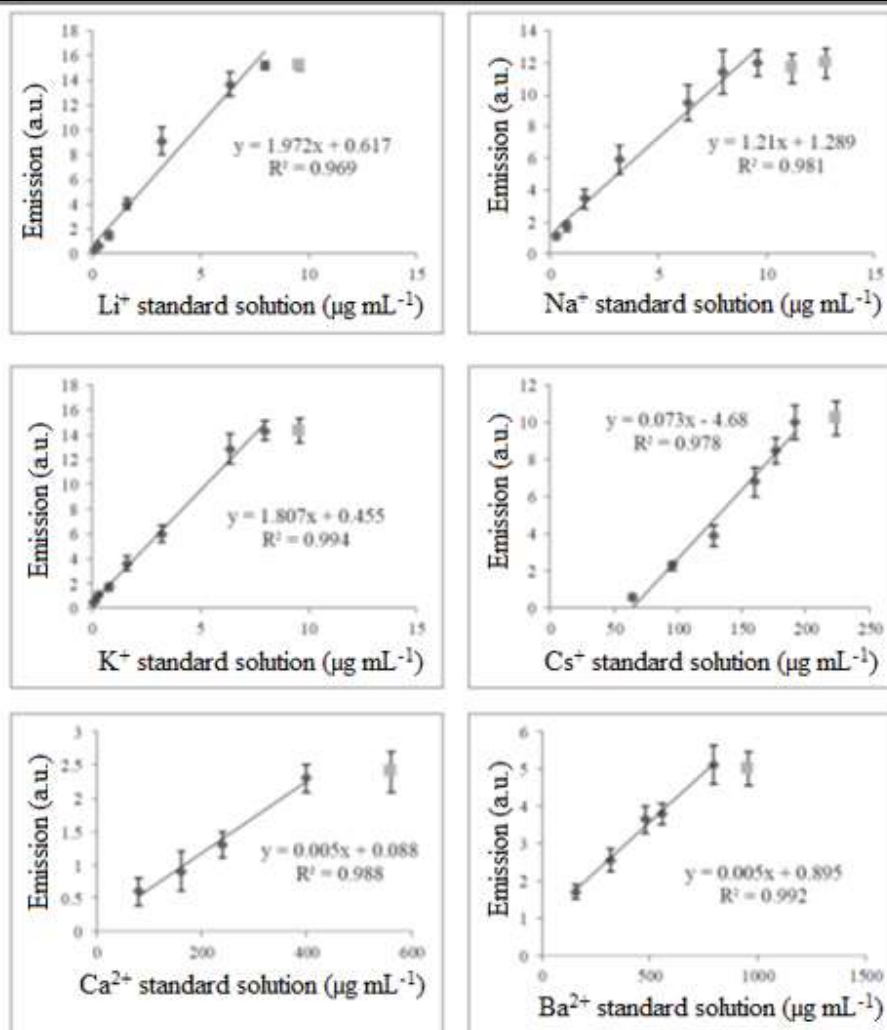


Fig. 7: Calibration curves for different metal ions using HCl (0.45 M) as a hydrogen radical generator.

Table.1: Optimized parameters during analysis of Li, Na, K, Cs, Ca and Ba by AESE.

| Species | Applied potential<br>(V, $\pm S$ , n=3) | Flow rate<br>(mL min <sup>-1</sup> , $\pm S$ , n=3) |                | Wavelength<br>(nm) [30] |
|---------|---|---|----------------|-------------------------|
|         |   | Air   | H <sub>2</sub> |                         |
| Li      | -100.0 $\pm$ 1.0                        | 142 $\pm$ 1   | 683 $\pm$ 1    | 670.8 $\pm$ 0.1         |
| Na      | -90.0 $\pm$ 1.0                         | 25 $\pm$ 1  | 560 $\pm$ 1    | 589.0 $\pm$ 0.1         |
| K       | -50.0 $\pm$ 1.0                         | 101 $\pm$ 1   | 560 $\pm$ 1    | 766.0 $\pm$ 0.1         |
| Cs      | -90.0 $\pm$ 1.0                         | 4 $\pm$ 1   | 560 $\pm$ 1    | 852.1 $\pm$ 0.1         |
| Ca      | -100.0 $\pm$ 1.0                        | 313 $\pm$ 1   | 683 $\pm$ 1    | 422.7 $\pm$ 0.1         |
| Ba      | -160.0 $\pm$ 1.0 V                      | 419 $\pm$ 1   | 560 $\pm$ 1    | 553.6 $\pm$ 0.1         |

Table.2: Figures of merit during analysis of alkali ions by the atomic emission spectroelectrochemistry.

| Metal ions       | Linear dynamic range<br>( $\mu\text{g mL}^{-1}$ ) | Correlation coefficient<br>(R, $\pm S$ , n=3) | Detection limit<br>( $\mu\text{g mL}^{-1}$ , $\pm S$ , n=3) |
|------------------|---|---|---|
| Li <sup>+</sup>  | 0.30- 8.0   | 0.984 $\pm$ 0.002                             | 0.070 $\pm$ 0.008   |
| Na <sup>+</sup>  | 0.26- 9.6   | 0.990 $\pm$ 0.003                             | 0.090 $\pm$ 0.005   |
| K <sup>+</sup>   | 0.65-8.0  | 0.997 $\pm$ 0.003                             | 0.040 $\pm$ 0.002   |
| Cs <sup>+</sup>  | 65.0- 192.0                                       | 0.989 $\pm$ 0.002                             | 40.0 $\pm$ 0.1  |
| Ca <sup>2+</sup> | 80.0-400.0  | 0.993 $\pm$ 0.005                             | 60.0 $\pm$ 0.2  |
| Ba <sup>2+</sup> | 160.0- 800.0                                      | 0.996 $\pm$ 0.004                             | 70.0 $\pm$ 0.2  |

Table.3: Real sample analyses.

| Real sample     | Atomic emission spectroelectrochemistry ( $\mu\text{g mL}^{-1}$ , $\pm S$ , n=3) |                 | ICP ( $\mu\text{g mL}^{-1}$ , $\pm S$ , n=3) |                 | Absolute error ( $\mu\text{g mL}^{-1}$ ) |        |
|-----------------|--|-----------------|--|-----------------|--|--------|
|                 | Na   | K               | Na   | K               | Na                                       | K      |
| Drinking water  | 9.81 $\pm$ 0.02  | 0.48 $\pm$ 0.05 | 10.10 $\pm$ 0.04                             | 0.40 $\pm$ 0.06 | 0.29                                     | -0.079 |
| Rain water      | 0.57 $\pm$ 0.02  | 0.46 $\pm$ 0.07 | 1.00 $\pm$ 0.04                              | 0.36 $\pm$ 0.05 | 0.43                                     | -0.105 |
| Dill distillate | 0.31 $\pm$ 0.04  | 0.28 $\pm$ 0.02 | 0.94 $\pm$ 0.08                              | 0.11 $\pm$ 0.04 | 0.63                                     | -0.165 |

Table.4: Comparison between some figures of merit between present study and previously reported methods for alkali ions detection.

| Analytical method   | Detection limit ( $\mu\text{g mL}^{-1}$ )   | Analyzed sample               | Dynamic range   | Reference |
|---|---|-------------------------------|---|-----------|
| Atomic emission using low-power capacitively coupled plasma microtorch and microspectrometer (Li) | 0.013 $\mu\text{g L}^{-1}$<br>( $1.3 \times 10^{-5} \mu\text{g mL}^{-1}$ )  | Drinking water                | 0.4–2140 $\mu\text{g L}^{-1}$<br>( $0.4 \times 10^{-3}$ - $2140 \times 10^{-3} \mu\text{g mL}^{-1}$ )                                     | [27]      |
| Ion chromatography(Na)  | 3.2 ng $\text{L}^{-1}$<br>( $3.2 \times 10^{-6} \mu\text{g mL}^{-1}$ )  | Potter plant samples          | 25-250 ng $\text{L}^{-1}$<br>( $25 \times 10^{-6}$ - $250 \times 10^{-6} \mu\text{g mL}^{-1}$ )   | [28]      |
| Flow-injection system with tubular ion-selective electrodes (K)                                   | $9.6 \times 10^{-6} \text{ mol L}^{-1}$<br>(0.375 $\mu\text{g mL}^{-1}$ )   | Concentration water samples   | $1.0 \times 10^{-5}$ to $1.0 \times 10^{-1} \text{ mol L}^{-1}$<br>(0.391-3909.83 $\mu\text{g mL}^{-1}$ )                                 | [29]      |
| Flow-injection system with tubular ion-selective electrodes (Ca)                                  | $5.6 \times 10^{-6} \text{ mol L}^{-1}$<br>(0.2244 $\mu\text{g mL}^{-1}$ )  | Concentration water samples   | $1.0 \times 10^{-5}$ to $1.0 \times 10^{-1} \text{ mol L}^{-1}$<br>( $40.078 \times 10^{-2}$ - $40.078 \times 10^2 \mu\text{g mL}^{-1}$ ) | [29]      |
| ICP-OES   | $0.06 \times 10^{-3}$ , $0.2 \times 10^{-3}$ , $0.3 \times 10^{-3}$ , $0.8 \times 10^{-3}$ , $0.03 \times 10^{-3}$ for Li, Na, K, Ca, Ba respectively ( $\mu\text{g mL}^{-1}$ ) | ---                           | ---   | [30]      |
| Atomic Absorption   | ---   | ---                           | (0.02-5 Li), (0.02-5 Na), (0.03-2.0 K), (0.04-5 Cs), (0.01-3 Ca), (0.02-50 Ba) $\mu\text{g mL}^{-1}$                                      | [30]      |
| Present study   | 0.07 for Li, 0.09 for Na, 0.04 for K, 40.0 for Cs, 60.0 for Ca, 70.0 for Ba ( $\mu\text{g mL}^{-1}$ )   | Drinking water and rain water | 0.30- 8.0 for Li, 0.26- 9.6 for Na, 0.65-8.0 for K, 65.0- 192.0 for Cs, 80.0-400.0 for Ca, 160.0- 800.0 for Ba ( $\mu\text{g mL}^{-1}$ )  | ---       |